forests

MDPI

Article

Effects of the Surface Roughness of Six Wood Species for Furniture Production on the Wettability and Bonding Quality of Coating

Qinglin Yu [1,2], Xi Pan [1,2], Zhong Yang [1,2,*], Li Zhang [1,2] and Jingyun Cao [1,2]

[1] Research Institute of Wood Industry, Chinese Academy of Forestry, Beijing 100091, China; yql9899@163.com (Q.Y.); xi__pan@163.com (X.P.); zl1534@outlook.com (L.Z.); cjy252114@163.com (J.C.)
[2] Key Laboratory of Wood Science and Technology, National Forestry and Grassland Administration, Beijing 100091, China
* Correspondence: zyang@caf.ac.cn; Tel.: +86-1062889432

Abstract: Wood surface roughness, surface free energy (SFE), wettability, and bonding quality for water-based acrylic coatings were investigated. The samples tested in this study included *Pinus radiata*, *Pinus sylvestris*, Larch, Hemp oak, Catalpa tree, and Camphor. Sandpaper with grits of 180, 240, 320, 400, and 500 was utilized to sand wood surfaces. The van OSS-Chaudhury-Good equation (vOCG) was used to calculate the SFE values. The modified model (M-D) was used to calculate the wettability based on the contact angle change rate (K value). The higher the K value, the faster the contact angle approaches equilibrium. A cross-cut test was used to evaluate the coating's bonding quality. The anatomical structure of wood has an impact on the roughness of hardwood. The equilibrium contact angle is influenced by the wood species and sandpaper grit size. Sanding can make the surface of wood more wettable. Radiata pine that had been sanded to 180 grit had the highest SFE value. After finishing with waterborne acrylic, hardwood had a slightly better coating adhesion than softwood. Hemp oak wood had the lowest coating adhesion (0.6) and the highest K value (0.82). The best bonding quality (0.4) was supplied by the camphor wood with the lowest K value (0.13). Wettability in terms of K values was a good indication of determining the bonding quality of the water-based acrylic coatings.

Keywords: furniture wood; surface roughness; surface free energy; wettability; waterborne acrylic; bonding quality

Citation: Yu, Q.; Pan, X.; Yang, Z.; Zhang, L.; Cao, J. Effects of the Surface Roughness of Six Wood Species for Furniture Production on the Wettability and Bonding Quality of Coating. *Forests* **2023**, *14*, 996. https://doi.org/10.3390/f14050996

Academic Editor: Sofia Knapic

Received: 13 April 2023
Revised: 23 April 2023
Accepted: 3 May 2023
Published: 11 May 2023

1. Introduction

Demand for wood as a raw material continues to increase the production of processed timber such as plywood, particleboard, and veneer lumber. As a result of its durability, environmental friendliness, and often pleasing appearance, wood is still an attractive option for the production of furniture. The six wood species (*Pinus radiata*, *Pinus sylvestris*, Larch, Hemp oak, Catalpa, and Camphor) for furniture could be utilized extensively for a variety of applications. Due to their straight and homogeneous textures, *Pinus radiata*, *Pinus sylvestris*, and Larch are frequently used for furniture and interior decorating [1,2]. Hemp oak has high density and good hardness [3]. Catalpa wood is resistant to decay and has a pretty straight grain with attractive patterns, so it is often utilized for high-quality wood furniture [4]. The exceptional material quality of camphor wood makes it a popular material for wardrobe construction [5]. There is a wealth of information available regarding this wood's mechanical, physical, and chemical characteristics. Their performance on the surface, however, has not yet been thoroughly investigated. The processing capabilities of wood products, such as wood coating, engineered wood panel bonding, and composite wood thermal treatment, depend on their surface qualities [6–9]. Therefore, in order to

increase the performance of wood coatings, the wettability of the six kinds of wood for furniture must be investigated.

The application of coatings such as varnish and white paint to wood surfaces is a standard practice in the furniture manufacturing process. The coating both enhances and preserves the surface of the wood. The varnish coating offers the furniture a higher gloss while preserving the original elegance of the grain of the wood surface and protecting it from insects, abrasion, and moisture. The white paint layer also conceals the texture and color flaws in wood, which are present in some wood products. Wood is protected from environmental factors such as moisture, weather, air, temperature, and sunshine by the coating [10–12].

The quality of finished wood products is greatly influenced by surface qualities. According to Candan and Darmawan et al., the contact angle decreases when the surface roughness increases, and then the wettability and bonding performance are improved [13,14]. Sanding influences surface roughness, which in turn impacts wettability [15,16]. Wettability can be obtained by measuring the contact angle between a droplet and the wood surface. Contact angles less than 90° indicate high wettability, where the liquid may effectively wet the surface of the wood. Contact angles greater than 90° indicates low wettability, in which the liquid is unable to adequately wet the surface of wood [17]. Sessile drops, captive bubbles, and the Washburn method are just a few of the many techniques that have been used to determine the contact angle of a surface [18–22]. Surface free energy is an important parameter to support information on interactions between wood surfaces and liquids (such as water, formamide, and diiodomethane). The SFE of wood has been evaluated using a wide range of models [8,23,24].

The durability of the coating film is determined by the bonding quality between the coating and the surface of the wood. One of the indicators of the quality of bonding is the ease with which sealer liquid wets the wood surface (wettability). Various models have been created by numerous scholars to evaluate the wettability of wood. Shi et al. proposed the S-D model, which was often used to evaluate dynamic wettability [25]. The " contact wetting rate angle" of the CRWA model was considered as the value determined when the wetting rate becomes constant [26]. The Shi-Gardner wetting model (S/G model) was introduced to evaluate the dynamic wetting process [25]. A modified wetting model was also developed by adding constraints on the initial and equilibrium contact angles [6].

Most research on wettability has been carried out on adhesives on woods and engineered boards [13,17,27,28]. However, there have been few investigations into the wettability of varnish or paint coatings on wood surfaces. This study's objectives were to assess the dynamic wettability of varnish sealers, determine the bonding quality of the varnish coating films, and analyze and compare the wettability of several furniture woods with various surface roughnesses.

2. Materials and Methods

2.1. Sample Preparation

Lumbers used for this study were six furniture species: *Pinus radiata* (*P. radiata*), *Pinus sylvestris* (*P. sylvestris* var. *mongolica* Litv.), Larch (*L. gmelinii*), Hemp oak (*Quercus-acutissima* Carr.), Catalpa (*Catalpa bungei* C.A.Mey), and Camphor (*C. longepaniculatum* (Gamble) N. Chao). The densities of the wood sample material were 0.391 g/cm^3, 0.572 g/cm^3, 0.530 g/cm^3, 0.896 g/cm^3, 0.511 g/cm^3, and 0.532 g/cm^3, respectively.

The lumbers were sliced at their surfaces in the molder. The samples were sawn by bandsaw in such a manner that tangential timbers were produced. Prior to the roughness and wettability tests, the samples were cut to produce the dimensions of 100 m × 58 mm × 8 mm (longitudinal × tangential × radial) and then placed in an air-conditioned chamber at 20 °C and a relative humidity of 65% for two weeks.

The paint used for the wettability test was a water-based acrylic sealer. The sealer (WDP300), primer (KGD-E34-101), and topcoat (KGM-E91-101) were supplied by Guangdong Haishun New Material Technology Co., Ltd., Foshan, China. The solid contents of

sealer, primer, and topcoat were 25.20%, 56.30%, and 47.16%, respectively. The viscosities of sealer, primer, and topcoat measured by a viscometer were 15, 80, and 70 mPa·s, respectively. Distilled water was purchased from Shenzhen Watsons Distilled Water Co., Ltd., Shenzhen, China. Diiodomethane and formamide were purchased from Shanghai Macklin Biochemical Technology Co., Ltd., Shanghai, China. The sandpapers with various grits required in the sanding process were supplied by Kraftwelle Industrial Co., Ltd., Hangzhou, China.

2.2. Surface Roughness Test

Sandpapers of different grits (P180, P240, P320, P400, and P500) were selected to be sanded 140–150 times along fiber direction within 1 min by hand, and the wood chips were cleaned up with a high-pressure air gun after sanding. The tangential lumber has provided a better decorative appearance, especially for furniture products coated with varnish. The measurement of surface roughness of wood specimens was performed perpendicular to the fiber direction at three different positions on the tangential surface of each sample using an ultra-depth three-dimensional microscope (VHX-6000, Keyence) according to ISO 25178-71: 2017 [29]. The value evaluated was the arithmetic mean roughness (Sa). The area was 2 mm^2, and the magnification of the optical microscope was 500 times.

2.3. Contact Angle Measurement

The dynamic contact angles of selected standard liquids (water, diiodomethane, and formamide) for measurement of SFE and of acrylic paint for measurement of wettability were measured with the contact angle tester with a high CCD camera (SPCA-X3, Harke, Beijing, China). The wood samples were set up on the stage in front of the CCD camera for measuring. An automatic syringe was used to drop specified standard liquids and acrylic paint in drops of 2 µL and 7 µL, respectively. The CCD camera recorded the drop shapes on the wood surface for a total of 30 s. For the purposes of measuring the contact angle, three droplets from each sample of standard liquids and acrylic paint were collected. At intervals of 2 s, for a total of 30 s, each video image was split into its own separate frame. The contact angle (θ) of each individual image of the drop was measured using the Contact Angle program. Each droplet contact angle with the surface of the wood samples was measured from both the left and the right side, and then the values were averaged. On the tangential surface of the wood samples, contact angles were averaged over three different points to reflect measurements over the entire surface. The contact angle tests were performed at room temperatures of 25 ± 2 °C with a relative humidity of 40 ± 2%.

2.4. Determination of Equilibrium Contact Angle and Constant Contact Angle Change Rate

To determine the equilibrium contact angle (θ_e) value, a segmented regression model was used. It was presumed that a function of the curve can adequately explain the changing contact angle during the wetting process (Figure 1). Over the initial stages of spreading and penetration, the function has a sharp slope; however, the later stages of the curve have a constant slope (plateau). Using Origin 8.0 nonlinear least-squares techniques, the function was directedly obtained (OriginLab, Northampton, MA, USA).

The contact angle at a specific time determines the contact angle change rate. In this study, the wettability was quantitatively assessed using the contact angle change rate (K-value) using the M-D model, which was modified by the Shi and Gardner (S/G) model [6]. The equation of the M-D model can be expressed as follows:

$$\theta = B + A \times e^{-Kt} \quad (1)$$

where θ is the contact angle at a certain time, when t = ∞, B is the equilibrium contact angle, when t = 0, $B + A$ is the initial contact angle, K is the constant contact angle change rate, and t is the wetting time.

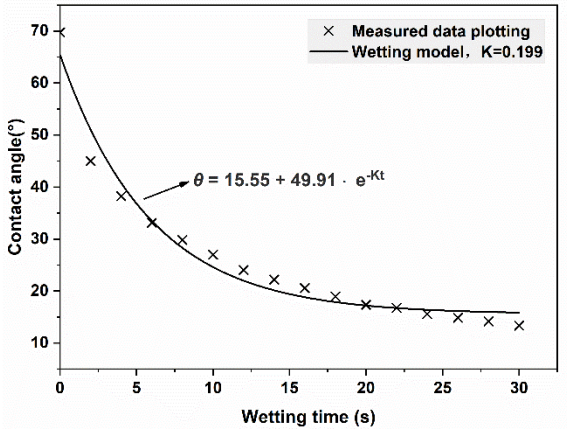

Figure 1. Determination of the equilibrium contact angle (θ_e) from a plot of the contact angle as a function of time by M-D model.

2.5. Determination of Surface Free Energy Components

The SFE of wood has been determined using a variety of techniques. The three-liquid method is modified to be a multi-liquid method to determine the SFE value, and its components are purposefully chosen using vOCG Equation (2).

$$\gamma_L(1+\cos\theta_e) = 2\sqrt{\gamma_s^{LW}\gamma_L^{LW}} + 2\sqrt{\gamma_s^{+}\gamma_L^{-}} + 2\sqrt{\gamma_s^{-}\gamma_L^{+}} \quad (2)$$

where γ_L is the total surface free energy of wood samples, θ_e is the equilibrium contact angle, γ_s^{LW} is the dispersive component of SFE, γ_L^{LW} is the dispersive surface tension, γ_s^{+} is the alkaline component of SFE, γ_s^{-} is acid component of SFE, γ_L^{-} is alkaline surface tension, γ_L^{+} is acid surface tension. The values of standard liquids are shown in Table 1.

Table 1. Surface tension and its components in the standard liquids.

Liquids	Surface Tension and Its Components (mJ/m^2)				
	γ_L	γ_L^{LW}	γ_L^{AB}	γ_L^{+}	γ_L^{-}
Water	72.8	21.8	51.0	25.5	25.5
Diiodomethane	50.8	50.8	0.0	0.0	0.0
Formamide	58.0	39.0	19.0	2.28	39.6

2.6. Coating Application and Bonding Test

The 320 grit-sanded wood samples were coated with the abovementioned varnish types for bonding quality evaluation. A hand-held electric spray gun was employed during the coating procedure (PQ40202BL, Zhejiang Bolai Electronic Technology Co., Ltd., Wenzhou, China). The ideal vertical distance between the spray gun and the wood surface was 200 mm, and the diameter of the spray gun nozzle was 1.8 mm. Following 2.5 h of drying at 25 degrees Celsius, the samples were lightly sanded with a 400 grit sandpaper, and the dust was subsequently cleaned using a high-pressure air gun purge. Three coating layers were applied to the wood surfaces, with a liquid application of 120 g/m^2 for each layer. All finished samples were used for performance tests after 7 days.

To evaluate the resistance of the coating films to separation from wood surfaces, a cross-cut tape test method was applied according to GB/T 4893.4-2013 [30]. A cross-cut pattern was made through the film using a sharp cutter head. After that, the incision was taped using pressure-sensitive adhesive. Using a hand or an eraser, the tape was smoothed over the cut area before quickly bringing it back over itself at an angle of around 180 degrees. Bonding quality was rated on a scale of 0 to 5; it is important to note that 5 represents 0% area removal and 0 represents more than 65% area removal. For each coating, five scales per sample were tested. The adhesion scales were subsequently averaged.

2.7. Statistics Analysis

The influence of wood species, liquid type, and sandpaper grit size on the wettability (equilibrium contact angle) between coatings and wood samples was examined using an ANOVA ($p < 0.05$). S-N-K tests were performed to identify significant differences between the average values of the factors.

3. Results and Discussion

3.1. Surface Roughness

Surface roughness is a crucial aspect of surface quality and plays a vital role in the production of wood products [31]. The sanding process has an impact on the wood's surface roughness as well. After slicing or sanding, wood cells are exposed on the cut surface, and the arrangement of the cellular tissue varies considerably depending on the anatomical structure of the wood [32]. The result in Table 2 shows that the mean values of surface roughness and densities of different specimens varied.

Table 2. Average surface roughness and density of six wood species.

Wood Species	Density (g/cm^{-3})	Sa (μm)				
		P180	P240	P320	P400	P500
Pinus radiata	0.391 ± 0.014	4.620 ± 0.229	5.170 ± 0.983	2.853 ± 0.114	2.363 ± 0.459	2.170 ± 0.411
Pinus sylvestris	0.572 ± 0.051	4.040 ± 0.539	5.213 ± 0.340	5.227 ± 0.981	2.330 ± 0.348	2.017 ± 0.191
Larch	0.530 ± 0.051	3.803 ± 0.896	4.417 ± 0.666	3.263 ± 0.312	3.277 ± 0.660	3.087 ± 0.701
Hemp oak	0.896 ± 0.047	3.517 ± 0.499	3.277 ± 0.186	4.460 ± 1.064	1.763 ± 0.363	4.237 ± 1.315
Catalpa	0.511 ± 0.047	3.827 ± 0.506	7.993 ± 2.634	3.520 ± 1.088	6.227 ± 4.498	8.403 ± 2.239
Camphor	0.532 ± 0.024	3.330 ± 0.519	3.833 ± 0.216	2.507 ± 0.460	3.370 ± 0.894	2.993 ± 0.251

In general, softwood specimens had a smoother surface after the sanding process than hardwood specimens. The larger the grit size, the smoother the wood surface. Several researchers came to the same conclusion [15,33]. Maximum Sa (5.170 μm, 4.417 μm) values for Larch and *Pinus radiata* were at 240 grits, while a minimum Sa values (2.170 μm, 3.087 μm) were obtained at 500 grits. The value of roughness of *Pinus sylvestris* was at a minimum at a P500 of 2.017 μm and reached a maximum at a P320 of 5.227 μm. Hemp oak sanded with P400 had the smoothest surface with a Sa value of 1.763 μm and Catalpa sanded with P500 had the roughest surface with a Sa value of 8.403μm. Surface roughness was also influenced by density, which varied greatly among species. After sanding with the same grit of sandpaper, the values of surface roughness (Sa) increased as the density of the wood decreased. After being sanded using a 180 grit sandpaper, the *Pinus radiata* with the lowest density (0.391 ± 0.014 g/cm^{-3}) exhibited the greatest degree of roughness (4.620 ± 0.229 μm). Otherwise, Hemp oak with the maximum density (0.896 ± 0.047 g/cm^{-3}) had minimal roughness (3.517 ± 0.499 μm). However, it is not always the case that the surface roughness will decrease with increasing sandpaper grit size. The microstructure of wood such as vessels has an effect on surface roughness, and the roughness of the part with obvious microstructure is 2–3 times larger than the inconspicuous parts [34]. At 400 and 500 grit sandpaper sizes compared to other grit sizes, the surface Sa of the Catalpa was much higher. Figure 2 shows the morphological characteristics of Catalpa after being sanded using P400 and P500 grain sandpaper. The results indicate that there is a substantial difference in the roughness of surfaces sanded with the same grit size in different areas. This difference is more pronounced in hardwood, which has more complex and diverse anatomical structures. The surface became rougher after sanding because longitudinal grooves and cracks were exposed. Figure 3 demonstrates the morphological characteristics of Larch that have been sanded with P320, P400, and P500. The surface morphology and surface roughness of Larch showed no significant variances after sanding with three different grit sizes. The homogenous structure of softwood makes the differences insignificant.

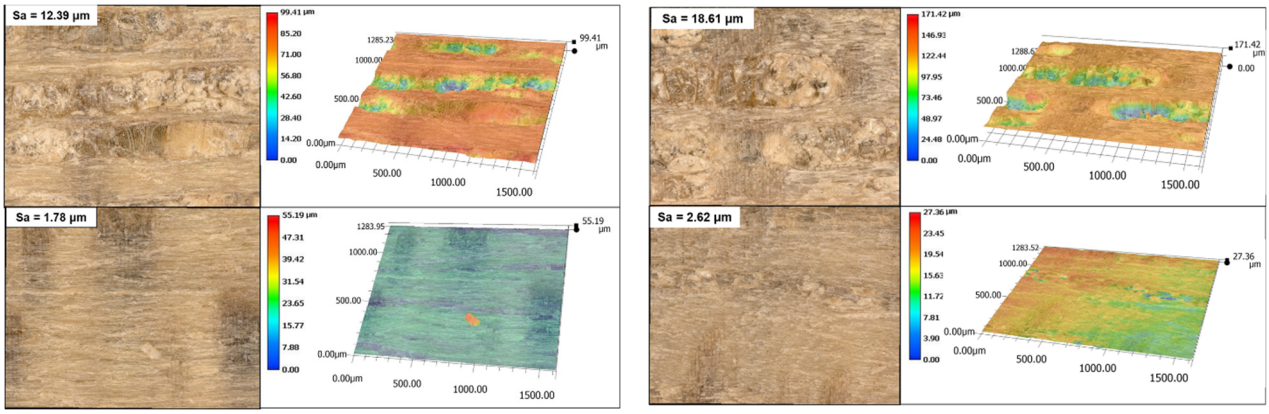

Figure 2. Surface topography and roughness of Catalpa (**a**) sanded P400, (**b**) sanded P500.

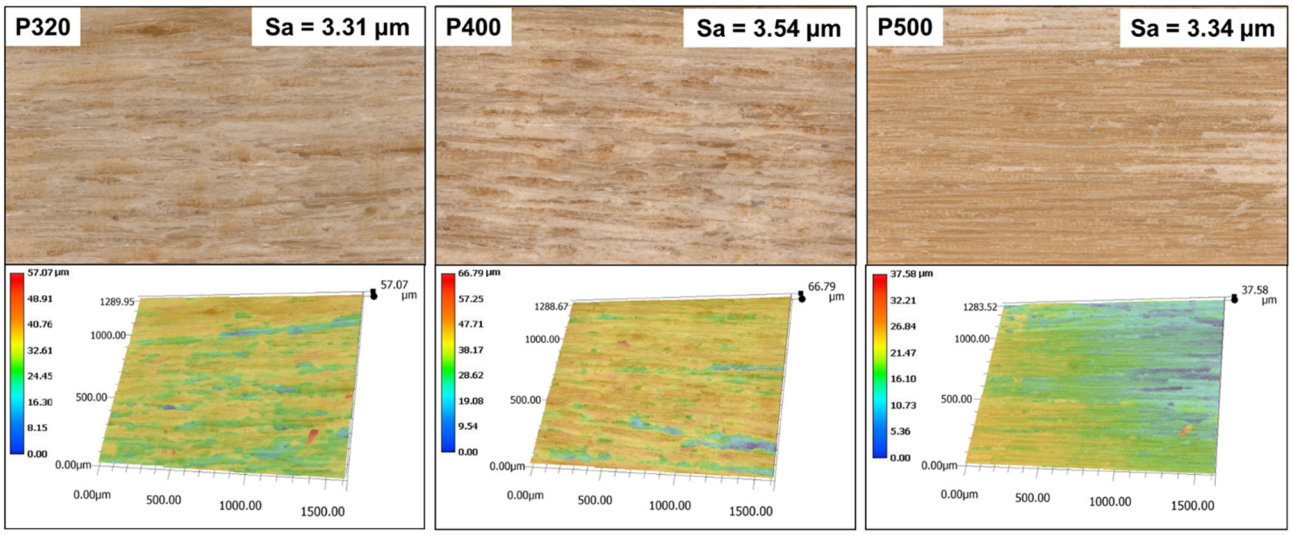

Figure 3. Surface topography and roughness of larch wood P320, P400, and P500 sanded.

3.2. Equilibrium Contact Angle

The results in Table 3 show the equilibrium contact angle values (θ_e) of six wood surfaces after sanding at different grit sizes. Among the woods without sanding, *Pinus radiata* had the minimum θ_e of 21.09°; Camphor had the largest θ_e of 63.85°. θ_e was significantly reduced after treatment, which indicated that sanding might improve the wettability of the wood surface. According to many studies, wood's surface hydrophilicity improved with increasing surface roughness. The surface wettability increased with decreasing water contact angle [35]. θ_e increased as the grit size increased in the range of 180 to 320 grit; however, when the grit sizes increased to P400 and P500, the variation of θ_e decreased. The water contact angle decreases as the surface becomes smoother and more hydrophilic reactive groups (such as hydroxyl groups) are exposed on the surface. Moreover, the residual wood dust is collected on the surface, lowering the contact angle. Several investigations have come to similar conclusions, showing that smooth wood surfaces exhibit hydrophilic properties [36]. *Pinus sylvestris*, in particular, showed a greater water contact angle than the other species. As a result of the resin in the wood moving to the surface after sanding because it includes a significant amount of hydrophobic resin, the surface becomes less wettable.

Table 4 shows that grit size and droplet type had a highly significant effect on the test ($P_r < 0.01$), and wood species had a significant effect on the equilibrium contact angle ($P_r < 0.05$). The droplet type, grit size, and wood species can be used to rank the variables

that affect the equilibrium contact angle of the wood surface using the *F*-value. The equilibrium contact angles of the sanded wood surface were much lower than those of the untreated wood, showing that sanding can effectively increase the wettability of the surface. The surface shows the minimum equilibrium contact angle when sanding with P180. It revealed that 180 grit sanding produced the highest wettability.

Table 3. Contact of angle of the sanded wood samples.

Wood Sample	Surface Pattern and Sanding Treatment	Equilibrium Contact Angle (°)		
		Water	Formamide	Diiodomethane
Pinus radiata	Control	21.09	0.55	16.51
	Sanded P180	4.53	4.38	11.51
	Sanded P240	9.41	0.69	9.23
	Sanded P320	15.55	0.85	16.08
	Sanded P400	17.72	2.42	27.14
	Sanded P500	14.43	1.44	19.83
Pinus sylvestris	Control	38.67	2.32	10.48
	Sanded P180	48.18	10.47	10.81
	Sanded P240	58.16	3.31	17.38
	Sanded P320	54.16	11.00	14.34
	Sanded P400	57.97	9.34	13.81
	Sanded P500	72.55	5.97	17.45
Larch	Control	51.38	13.27	27.77
	Sanded P180	4.56	0.41	14.12
	Sanded P240	12.24	1.27	17.37
	Sanded P320	17.25	1.66	24.40
	Sanded P400	18.46	2.51	24.32
	Sanded P500	19.87	0.88	20.82
Hemp oak	Control	46.93	7.16	31.65
	Sanded P180	18.31	1.6	29.66
	Sanded P240	18.29	2.86	26.59
	Sanded P320	23.66	3.51	22.18
	Sanded P400	25.13	5.67	29.97
	Sanded P500	26.03	5.27	35.04
Catalpa	Control	51.05	25.99	42.95
	Sanded P180	23.71	7.35	30.64
	Sanded P240	24.23	7.50	33.00
	Sanded P320	34.15	11.32	34.86
	Sanded P400	34.13	14.82	35.04
	Sanded P500	37.22	10.77	36.33
Camphor	Control	63.85	29.38	46.18
	Sanded P180	34.03	6.28	45.69
	Sanded P240	26.64	6.09	38.86
	Sanded P320	41.87	11.52	40.29
	Sanded P400	28.77	9.33	40.60
	Sanded P500	34.49	12.36	43.49

Table 4. Analysis of variance for the equilibrium contact angle.

Source	Sum of Squares	DF	Mean Squares	*F*	Significance
Grit size	2204.902	5	440.980	4.906	0.003 **
Wood species	1332.640	5	266.528	2.965	0.033 *
Droplet type	2193.061	2	1096.530	12.199	0.000 **
Error	2067.457	23	89.889		
Corrected total	24,955.566	36			

* Significant at $\alpha = 5\%$; ** Significant at $\alpha = 1\%$.

3.3. Surface Free Energy

The SFE values of the wood samples are presented in Table 5. The highest surface free energy was found in a Pinus radiata sample that was not sanded and the lowest free energy was found in Camphor with values of 84.196 mJ/m^2 and 55.051 mJ/m^2, respectively. The highest surface free energy of 88.096 mJ/m^2, 87.392 mJ/m^2, 84.457 mJ/m^2, 81.051 mJ/m^2, and 84.129 mJ/m^2 were obtained for Pinus radiata after sanding with five grit sandpaper; The surface free energies of Camphor were all the lowest, 66.541 mJ/m^2, 73.179 mJ/m^2, 63.138 mJ/m^2, 71.537 mJ/m^2, and 67.173 mJ/m^2, respectively. The higher the surface free energy value of the wood, the higher the energy on the surface of the wood, and the faster the liquid diffused and penetrated the surface. The maximum SFE was attained while using an 180 grit sandpaper, with the control sample having a lower SFE value than the sanded samples. According to Sinn et al., an increase in wood roughness initially results in an increase in the SFE value, but when the value reaches a certain range, the SFE value decreases [16]. The SFE of *Pinus sylvestris* decreased after sanding, and the SFE value tended to decrease as the grit size increased. *Pinus sylvestris* wood contains an abundance of hydrophobic resin, which causes the resin to transfer to the surface after sanding and reduce the SFE and components. The surface roughness reduced, and the contact area of the droplets on the smooth wood surface shrank as the sanding grit increased [14]. The surface free energy was decreased at the same time that the wood voids were filled with wood dust [18].

Table 5. Surface-free energy and components for six furniture wood species.

Wood	Surface Pattern and Sanding Treatment	vOCG			
		γ^{LW} [1]	γ^{-} [2]	γ^{+} [3]	γ_s [4]
Pinus radiata	Control	48.727	32.216	3.253	84.196
	Sanded P180	49.784	34.237	4.076	88.096
	Sanded P240	50.144	33.210	4.037	87.392
	Sanded P320	48.832	31.186	4.439	84.457
	Sanded P400	45.359	30.132	5.560	81.051
	Sanded P500	47.832	31.559	4.738	84.129
Pinus sylvestris	Control	49.955	27.828	1.053	78.836
	Sanded P180	49.903	12.021	4.064	65.987
	Sanded P240	48.508	5.548	4.910	58.966
	Sanded P320	49.230	8.232	4.296	61.758
	Sanded P400	49.342	5.935	4.413	59.690
	Sanded P500	48.490	0.467	5.053	54.010
Larch	Control	45.116	23.339	0.444	68.899
	Sanded P180	49.277	34.042	4.279	87.598
	Sanded P240	48.509	32.335	4.522	85.366
	Sanded P320	46.365	30.370	5.224	81.959
	Sanded P400	46.391	29.872	5.210	81.473
	Sanded P500	47.537	29.240	4.861	81.638
Hemp oak	Control	43.527	24.788	1.105	69.420
	Sanded P180	44.362	29.789	5.930	80.081
	Sanded P240	45.570	29.914	5.482	80.966
	Sanded P320	47.111	27.370	4.984	79.465
	Sanded P400	44.234	26.543	5.918	76.695
	Sanded P500	42.012	25.869	6.792	74.672
Catalpa	Control	38.094	23.070	1.512	62.676
	Sanded P180	43.955	27.481	5.933	77.369
	Sanded P240	42.933	27.150	6.311	76.395
	Sanded P320	42.095	21.455	6.464	70.014
	Sanded P400	42.012	22.079	6.167	70.258
	Sanded P500	41.403	19.252	6.819	67.474

Table 5. *Cont.*

Wood	Surface Pattern and Sanding Treatment	vOCG			
		γ^{LW} [1]	γ^{-} [2]	γ^{+} [3]	γ_s [4]
Camphor	Control	36.374	18.408	0.269	55.051
	Sanded P180	36.640	20.660	9.241	66.541
	Sanded P240	40.181	25.475	7.523	73.179
	Sanded P320	39.466	16.043	7.630	63.138
	Sanded P400	39.305	24.505	7.727	71.537
	Sanded P500	37.815	21.159	8.199	67.173

[1] γ^{LW} is polar component of SFE; [2] γ^{-} is acid component of SFE; [3] γ^{+} is alkaline component of SFE; [4] γ_s is the value of total SFE.

The alkaline component values of the wood specimen were higher than its acidic component values. The same conclusions were reached by Gindl et al. [18]. The alkaline content of the wood declined, and the acid content gradually increased as the grit size grew. The acidic groups are produced by the migration of extractives to the wood surface following oxidation, whereas the basic groups are produced by the rearrangement of the groups between the wood and air. It indicated that the primary component influencing the surface chemistry of wood was extractives [37,38].

3.4. Wettability of Acrylic Paint

Figure 4 shows the contact angle and wetting time for water-based acrylic on 320 grit-sanded wood surfaces. Due to the water-based acrylic sealer spreading and penetrating the surface of the wood, all droplet contact angles decreased as the wetting duration increased. *Pinus radiata* had the least value, while Camphor had the maximum contact angle during the entire wetting process, indicating that the water-based acrylic sealer droplets spread more readily on the surface of *Pinus radiata* wood. The contact angle changed throughout the first two seconds on various wood surfaces, decreasing more quickly on the surface of Hemp oak and more slowly on the surface of camphor. Overall, softwood exhibited a higher wettability than hardwood, which was shown by the larger contact angles of the former.

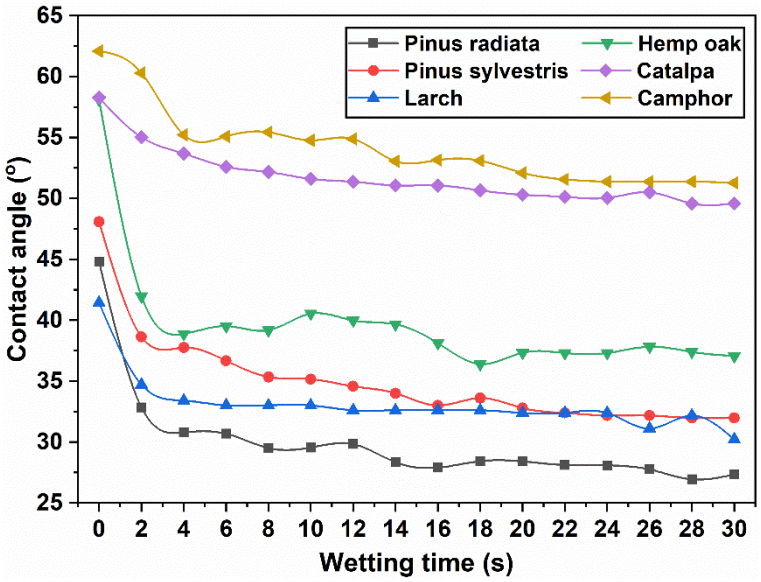

Figure 4. Progress of contact angle and wetting time for water-based acrylic on six wood surfaces.

A popular wood-wetting model is the M-D model. By using the M-D model, the wettability of the varnish layer on various wood surfaces may be quantitatively assessed. The speed at which the liquid spreads and permeates can be calculated using the K value.

As the contact angle approaches equilibrium more quickly, and the liquid spreads more quickly, the higher the K value [8]. All experimental data are included in Table 6, along with the constant contact angle change rates (K value). Figure 1 illustrates the wetting process of water-based acrylic using the M-D model on the tangential surface of 320 grit sanded *Pinus radiata* wood as an example of K value calculation. Table 6 shows the R squared values, errors, initial contact angles, equilibrium contact angles, and contact angle reduction ratio for all wood surfaces examined. R squared values of the wetting model were over 0.915 for all wood samples. Therefore, the M-D model could accurately be used to describe the varnish wetting process on the six wood surfaces. Moreover, Table 6 demonstrates that Hemp oak wood had the highest K value of 0.82, indicating that its surface was more wettable. The K value for camphor wood was the lowest at 0.13, meaning that water-based acrylic droplets dispersed slowly on the surfaces. Hemp oak wood has big vessels, which allow liquids to flow into the wood when they fall on surfaces, spread out quickly, and reach an equilibrium state.

Table 6. Nonlinear fitting results for water-based acrylic on six wood surfaces.

Wood Sample	K Value	R^2	Errors	Initial Contact Angle (°)	Equilibrium Contact Angle (°)	Contact Angle Reduction Ratio (%)
Pinus radiata	0.53	0.955	0.08	44.54	28.42	36.20%
Pinus sylvestris	0.25	0.936	0.04	46.78	32.77	29.95%
Larch	0.58	0.915	0.12	41.37	32.29	21.95%
Hemp oak	0.82	0.947	0.16	58.09	38.25	34.15%
Catalpa	0.17	0.976	0.02	57.81	50.06	13.41%
Camphor	0.13	0.926	0.03	61.64	51.31	16.76%

3.5. Bonding Quality

Table 7 presents the bonding qualities of six wood species. Table 7 demonstrates that hardwood has better adhesion than softwood. In comparison to other woods, Hemp oak gave the highest average bonding quality due to its vesicular structure and high K values (0.82). Anatomical structure would be one of the important factors affecting the bonding quality between the coating and the wood surface. The porous structure of Hemp oak wood allowed for increased coating absorption and penetration, which in turn improved bonding qualities. To produce a solid binding between the coating material and the wood surface, the coating liquid flowed and filled the vessel structure of the wood. The bonding quality average was lowest in *Pinus sylvestris* and Larch. According to Shi and Gardner et al., the higher the K value, the quicker the contact angle reached equilibrium and the quicker the liquids spread on the surface of the wood [25].

Table 7. Bonding quality and its mean scores for water-based acrylic coatings for six wood species.

Wood Sample	Bonding Quality	Mean Scores
Pinus radiata	0 (60%), 1 (40%)	0.4
Pinus sylvestris	0 (20%), 1 (80%)	0.8
Larch	0 (20%), 1 (80%)	0.8
Hemp oak	0 (80%), 1(20%)	0.2
Catalpa	0 (40%), 1 (60%)	0.6
Camphor	0 (60%), 1(40%)	0.4

The bonding quality of the coating initially declined and then increased as the total surface free energy and polar component increased. The wettability and bonding quality of the wood surface improved within a limited range as the SFE value increased.

4. Conclusions

Based on the findings of this work, the following general conclusions are noted. The value of surface roughness decreases as the grit sizes increase. The anatomical structure of the wood has an impact on surface roughness. The equilibrium contact angle is influenced by the types of sanding grits and the species of wood. Generally, sanding can make the surface of wood more wettable. The highest SFE value was produced by the 180 grit. The wettability and bonding quality of the wood surface improved within a limited range as the SFE value increased. The varnish wetting process on the six wood surfaces can be described by the wetting model's R squared values, which were over 0.915. Hardwood had a slightly better coating adhesion than softwood after finishing with water-based acrylic. Additionally, the Hemp oak with the best wettability can offer good water-based acrylic coating bonding qualities. The wettability in terms of K value is a good way to assess the bonding quality of a water-based acrylic coating.

Author Contributions: Conceptualization, Q.Y. and Z.Y.; software, Q.Y.; validation, X.P.; investigation, Q.Y.; data curation, Q.Y.; writing—original draft preparation, Q.Y.; writing—review and editing, Z.Y., L.Z. and J.C.; project administration, Z.Y. All authors have read and agreed to the published version of the manuscript.

Funding: This research were funded by the Fundamental Research Funds for Central Public Welfare Research Institutes (CAFYBB2021ZJ001) and the Key Research Funds of the Development Project Fund National Forestry and Grassland Administration (GLM [2021]13).

Data Availability Statement: No new data were created or analyzed in this study. Data sharing is not applicable to this article.

Acknowledgments: The authors thank Guangdong Haishun New Material Technology Co., Ltd., for the research support.

Conflicts of Interest: The authors declare no conflict of interest.

References

1. Jing, O.Y.; Jun, O. Factors Influencing the Surface Color Difference of Pinus sylvestris wood. *Furniture* **2021**, *42*, 26–30. [CrossRef]
2. Wei, S.; Junyi, Y.; Zairan, X.; Zhendong, X. New Zealand Radial Pine Import and Application Analysis. *Int. Wood Ind.* **2020**, *50*, 38–42.
3. Liu, Y.; Liu, Y.; Wei, Q.; Liang, B.; Zhao, J. Influence of Heat Treatment Temperature on Dimensional Stability of Sesquiterpene Wood. *J. Northeast. For. Univ.* **2022**, *50*, 99–101+118. [CrossRef]
4. Rui, W.; Lanlan, S.; YuronG, W. Rapid Prediction of Bending Resistance Properties of Liriodendron tulipifera Wood using NIR Spectroscopy. *Spectrosc. Spect. Anal.* **2023**, *43*, 557–562.
5. Fan, Z.; Huang, Z.; Huang, W.; Li, X.; Zhang, H. Comparison of Anatomical Characteristics of Five Species of Camphor wood in Sichuan. *Guangxi For. Sci.* **2022**, *51*, 411–416. [CrossRef]
6. Qin, Z.Y.; Liao, M.Y.; Zhang, Y.F.; Sun, J.P. Wood Interface and Surface Wettability Based on Contact Angle Method. *J. Beihua Univ. Nat. Sci. Ed.* **2019**, *20*, 249–255. [CrossRef]
7. Martha, R.; Dirna, F.C.; Hasanusi, A.; Rahayu, I.; Darmawan, W. Surface Free Energy of 10 Tropical Woods Species and Their Acrylic Paint Wettability. *J. Adhes. Sci. Technol.* **2019**, *34*, 167–177. [CrossRef]
8. Darmawan, W.; Nandika, D.; Noviyanti, E.; Alipraja, I.; Dumasari, D.; Gardner, D.; Gerardin, P. Wettability and Bonding Quality of Exterior Coatings on Jabon and Sengon Wood Surfaces. *J. Coat Technol. Res.* **2018**, *15*, 95–104. [CrossRef]
9. Croitoru, C.; Spirchez, C.; Lunguleasa, A.; Cristea, D.; Roata, I.C.; Pop, M.A.; Bedo, T.; Stanciu, E.M.; Pascu, A. Surface Properties of Thermally Treated Composite Wood Panels. *Appl. Surf. Sci.* **2018**, *438*, 114–126. [CrossRef]
10. Cogulet, A.; Blanchet, P.; Landry, V. The Multifactorial Aspect of Wood Weathering: A Review Based on a Holistic Approach of Wood Degradation Protected by Clear Coating. *BioResources* **2018**, *13*, 2116–2138. [CrossRef]
11. Cogulet, A.; Blanchet, P.; Landry, V.; Morris, P. Comparison of Exterior Coatings Applied to Oak Wood as a Function of Natural and Artificial Weathering Exposure. *Int. Biodeterior. Biodegrad.* **2018**, *129*, 33–41. [CrossRef]
12. De Windt, I.; Van den Bulcke, J.; Wuijtens, I.; Coppens, H.; Van Acker, J. Outdoor Weathering Performance Parameters of Exterior Wood Coating Systems on Tropical Hardwood Substrates. *Eur. J. Wood Prod.* **2014**, *72*, 261–272. [CrossRef]
13. Candan, Z.; Büyüksarı, U.; Korkut, S.; Unsal, O.; Çakıcıer, N. Wettability and Surface Roughness of Thermally Modified Plywood Panels. *Ind. Crops Prod.* **2012**, *36*, 434–436. [CrossRef]

14. Darmawan, W.; Ginting, M.; Gayatri, A.; Putri, R.; Dumasari, D.; Hasanusi, A. Influence of Surface Roughness of Ten Tropical Woods Species on Their Surface Free Energy, Varnishes Wettability and Bonding Quality. *Pigment. Resin Technol.* **2020**, *49*, 441–447. [CrossRef]
15. Hendarto, B.; Shayan, E.; Ozarska, B.; Carr, R. Analysis of Roughness of a Sanded Wood Surface. *Int. J. Adv. Manuf. Technol.* **2006**, *28*, 775–780. [CrossRef]
16. Sinn, G.; Gindl, M.; Reiterer, A.; Stanzl-Tschegg, S. Changes in the Surface Properties of Wood Due to Sanding. *Holzforschung* **2004**, *58*, 246–251. [CrossRef]
17. Iva Gavrilovic-Grmusa, I.; Dunky, M.; Miljkovic, J.; Djiporovic-Momcilovic, M. Influence of the Viscosity of UF Resins on the Radial and Tangential Penetration into Poplar Wood and on the Shear Strength of Adhesive Joints. *Holzforschung* **2012**, *66*, 849–856. [CrossRef]
18. Gindl, M.; Sinn, G.; Reiterer, A.; Tschegg, S. Wood Surface Energy and Time Dependence of Wettability: A Comparison of Different Wood Surfaces Using an Acid-Base Approach. *Holzforschung* **2001**, *55*, 433–440. [CrossRef]
19. Jankowska, A.; Zbiec, M.; Kozakiewicz, P.; Koczan, G.; Olenska, S.; Beer, P. The Wettability and Surface Free Energy of Sawn, Sliced and Sanded European Oak Wood. *Maderas Cienc. Tecnol.* **2018**, *20*, 443–454. [CrossRef]
20. Leggate, W.; Kumar, C.; McGavin, R.L.; Faircloth, A.; Knackstedt, M. The Effects of Drying Method on the Wood Permeability, Wettability, Treatability, and Gluability of Southern Pine from Australia. *BioResources* **2021**, *16*, 698–720. [CrossRef]
21. Liptáková, E.; Kúdela, J.; Bastl, Z.; Spirovová, I. Influence of Mechanical Surface Treatment of Wood on the Wetting Process. *Holzorschung* **1995**, *49*, 369–375. [CrossRef]
22. Kiesvaara, J.; Yliruusi, J. The Use of the Washburn Method in Determining the Contact Angles of Lactose Powder. *Int. J. Pharm.* **1993**, *92*, 81–88. [CrossRef]
23. Karlinasari, L.; Lestari, A.T.; Priadi, T. Evaluation of Surface Roughness and Wettability of Heat-Treated, Fast-Growing Tropical Wood Species Sengon (*Paraserianthes falcataria* (L.) I.C. Nielsen), Jabon (*Anthocephalus cadamba* (Roxb.) Miq), and Acacia (*Acacia mangium* Willd.). *Int. Wood Prod. J.* **2018**, *9*, 142–148. [CrossRef]
24. Wang, X.; Wang, F.; Yu, Z.; Zhang, Y.; Qi, C.; Du, L. Surface Free Energy and Dynamic Wettability of Wood Simultaneously Treated with Acidic Dye and Flame Retardant. *J. Wood Sci.* **2017**, *63*, 271–280. [CrossRef]
25. Shi, S.; Gardner, D. Dynamic Adhesive Wettability of Wood. *Wood Fiber Sci. J. Soc. Wood Sci. Technol.* **2001**, *33*, 58–68. [CrossRef]
26. Nussbaum, R.M. Natural Surface Inactivation of Scots Pine and Norway Spruce Evaluated by Contact Angle Measurements. *Holz. Roh. Werkst.* **1999**, *57*, 419–424. [CrossRef]
27. Baldan, A. Phenomena in Bonded Joints. *Int. J. Adhes.* **2012**, *38*, 95–116. [CrossRef]
28. Büyüksarı, Ü.; Avci, E.; Akkılıç, H. Effect of Pine Cone Ratio on the Wettability and Surface Roughness of Particleboard. *BioResources* **2014**, *5*, 1824–1833. [CrossRef]
29. *EN ISO 25178-71:2017*; Geometrical Product Specifications (GPS)—Surface Texture: Areal—Part 71. Software Measurement Standards: Geneva, Switzerland, 2017.
30. *GB/T 4893.4-2013*; Test of Surface Coatings of Furniture-Part 4: Determination of Adhesion-Cross Cut. GlobalSpec: Albany, NY, USA, 2013.
31. Büyüksarı, Ü.; Akbulut, T.; Guler, C.; As, N. Wettability and Surface Roughness of Natural and Plantation-Grown Narrow-Leaved ASH (Fraxinus Angustifolia Vahl.) Wood. *BioResources* **2011**, *6*, 4721–4730. [CrossRef]
32. Zhao, X. *Wood Finishing Process*; Chemical Industry Press: Beijing, China, 2006; pp. 22–24.
33. Fujiwara, Y.; Fujii, Y.; Okumura, S. Relationship between Roughness Parameters Based on Material Ratio Curve and Tactile Roughness for Sanded Surfaces of Two Hardwoods. *J. Wood Sci.* **2005**, *51*, 274–277. [CrossRef]
34. Long, Q.; Dong, X.; Zhefeng, L. Analysis of Cut Wood Surface Roughness Based on 3D Microscopic Systems. *China For. Prod. Ind.* **2020**, *57*, 13–17. [CrossRef]
35. Piao, C.; Winandy, J.E.; Shupe, T.F. From Hydrophilicity to Hydrophobicity: A Critical Review: Part I. Wettability and Surface Behavior. *Wood Fiber Sci.* **2010**, *42*, 490–510. [CrossRef]
36. Acda, M.N.; Devera, E.E.; Cabangon, R.J.; Ramos, H.J. Effects of Plasma Modification on Adhesion Properties of Wood. *Int. J. Adhes.* **2012**, *32*, 70–75. [CrossRef]
37. Gardner, D.J.; Wolcott, M.P.; Wilson, L.; Huang, Y.; Carpenter, M. *Our Understanding of Wood Surface Chemistry in 1995*; University of Wisconsin-Madison: Madison, WI, USA, 1995.
38. Wålinder, M.E.P. Study of Lewis Acid-Base Properties of Wood by Contact Angle Analysis. *Holzforschung* **2002**, *56*, 363–371. [CrossRef]